

Concrete modulus of rupture – analytical description of strength, size-effect and brittleness

C.V.Nielsen & N.Bicanic

University of Glasgow, Department of Civil Engineering, Glasgow, Scotland

ABSTRACT: An analytical model of bending of plain concrete beams is presented. Applying the fictitious crack model with a linear softening curve the moment-curvature relationship is obtained. The modulus of rupture is known to depend only on the initial slope of the σ - w curve. Hence, a linear softening model gives sufficient accuracy. The brittleness number, including beam size and softening characteristics, is shown to be the key parameter through which both small and large-size behaviour is modelled correctly. Comparisons with existing FEM-based expressions for the modulus of rupture show a good agreement.

1 INTRODUCTION

The modulus of rupture f_r measured from three- or four-point bending tests on plain concrete beams is often used to assess the uniaxial tensile strength f_t of concrete. These tests are easy to perform and there exists several standards for their execution (e.g. ASTM C78). However, experimental evidence shows that f_r is generally larger than f_t by about 25%, see e.g. Neville (1995).

Throughout the past 2 decades several investigations have considered bending of plain concrete beams by applying FEM with tensile softening material behaviour. For a general review see Planas et al. (1995) or the recent textbook by Bazant and Planas (1998). Alvaredo & Torrent (1987) suggested a major simplification of the problem, viz. that the modulus of rupture was governed only through the initial portion of the softening curve.

The basic finding of the FEM based investigations using various softening curves is that f_r is size dependent. However, this size-effect is different from the LEFM-size-effect, where strength is decreasing proportional to $D^{-1/2}$, where D is the beam depth. In LEFM the size-effect is linked with the existence of cracks/notches giving rise to stress singularities whereas the size-effect on f_r is due to the softening zone in the boundary layer, Bazant & Li (1995).

The present paper gives an analytical solution to the problem in accordance with the technical bending theory. The work is based on previous investigations by Chuang & Mai (1989) and by Ulfkjær et al. (1995). A general approach is taken, showing that the fictitious crack model and the crack band model

yield identical solutions to the problem. The analytical solution is compared with a FEM based expression and it is demonstrated that the analytical model agrees with this expression.

One may of course ask whether an analytical solution is needed when FEM based expressions are already available. There are several reasons for an analytical solution: (i) the solution is based on simple well-known assumptions, (ii) in addition to the strength, the solution also includes the depth of the fracture zone and the stress distribution, (iii) the solution is born with correct small- and large-size behaviour and (iv) a better understanding of the important parameters is achieved.

2 TENSION SOFTENING

When the tensile stress exceeds the uniaxial strength f_t concrete starts to crack. In a deformation controlled tensile test the complete load-elongation curve of a plain concrete sample shows an elastic phase governed by the modulus of elasticity E , until f_t is reached, followed by a decreasing curve (softening) where cracking takes place until the sample is completely separated in two halves.

The interpretation of the softening behaviour has mainly been divided in two research groups: (i) the fictitious crack model by Hillerborg et al. (1976) and (ii) the smeared crack band model by Bazant & Oh (1983). In Figure 1 the two models are outlined with linear softening for simplicity. The softening behaviour described by the two models is widely accepted to be identical, however, there are computational differences.

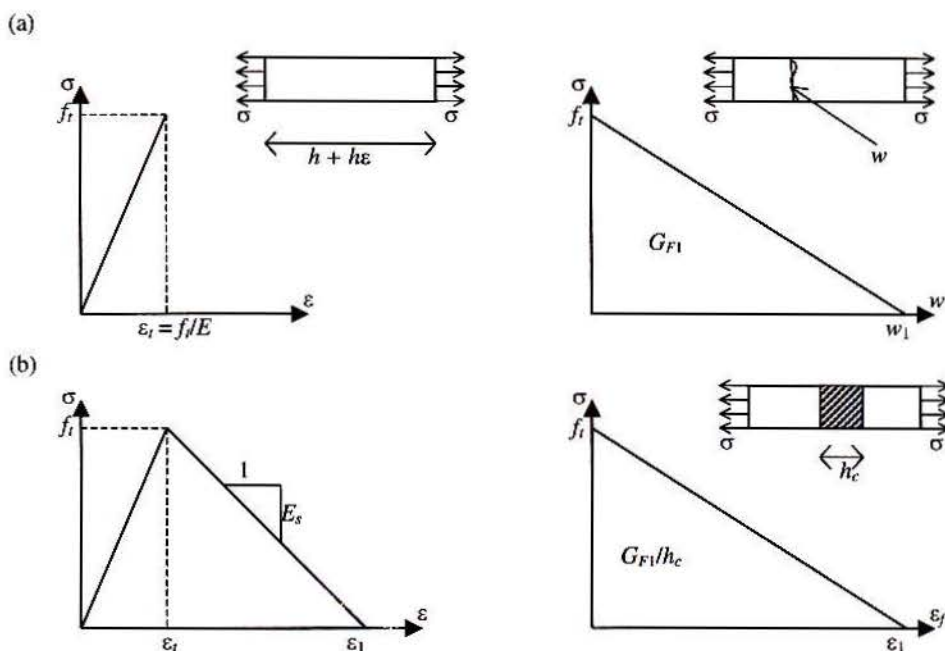


Figure 1. Linear softening models. (a) Fictitious crack model. (b) Crack band model.

2.1 Basic assumptions

From Figure 1 a few basic features for the softening curves are recovered. It is well known that the area under the σ - w curve equals the fracture energy G_F . For the linear softening we denote the fracture energy with subscript 1, $G_{F1} = f_t w_1 / 2$. The area under the σ - ϵ curve equals the fracture energy per volume in the crack band, i.e. in order to obtain identical fracture energies for the two models it follows

$$G_{F1} = \frac{1}{2} f_t w_1 = \frac{h_c}{2} f_t \epsilon_1 = \frac{h_c f_t^2}{2 E} \left(1 + \frac{E}{E_s} \right) = \frac{h_c f_t^2 \epsilon_1}{2 E \epsilon_t} \quad (1)$$

Note that the softening modulus E_s is treated as a positive value, contrary to the usual approach by Bazant.

Hillerborg defined a characteristic length $l_{ch} = EG_F/f_t^2$ as a material property. For the linear softening curve Alvarado & Torrent (1987) defined a similar characteristic length based only on the initial slope of the σ - w curve:

$$l_1 = \frac{EG_{F1}}{f_t^2} = \frac{E w_1}{2 f_t} = \frac{h_c E_s + E}{2 E_s} = \frac{h_c \epsilon_1}{2 \epsilon_t} \quad (2)$$

The initial portion of the softening curve is recognized to be of major importance to the modulus of rupture, i.e. it is sufficient to apply linear softening

when considering the modulus of rupture. Thus, the remaining part of the softening curve mainly affects the post-peak behaviour.

2.2 Brittleness number

In order to compare the two models further a simple example is investigated (Fig. 1). A specimen of length h is elongated until f_t is reached followed by softening either in a discrete crack or in a crack band of width h_c ($\leq h$). The post-softening elongation of the specimen is written as

$$\Delta h = h \epsilon = \begin{cases} \frac{\sigma(w)}{E} h + w \\ \frac{\sigma(\epsilon_f)}{E} h + h_c \epsilon_f \end{cases} \quad (3)$$

where subscript f denotes fracture strain. By inserting the following constitutive relationships

$$\sigma(w) = f_t \left(1 - \frac{w}{w_1} \right), \quad \sigma(\epsilon_f) = f_t - \frac{E_s E \epsilon_f}{E_s + E} \quad (4)$$

and rearranging, identical relationships between the localized elongation and the total elongation are obtained:

$$h(\varepsilon - \varepsilon_i) = \begin{cases} w \left(1 - \frac{hf_r}{Ew_1} \right) = w(1 - B) \\ h_c \varepsilon_f \left(1 - \frac{h}{h_c} \frac{E_s}{E_s + E} \right) = h_c \varepsilon_f (1 - B) \end{cases} \quad (5)$$

where the brittleness number B , as defined by Ulfkjaer et al. (1995), is inserted:

$$B = \frac{h}{2l_1}, \quad 0 \leq B \leq 1 \quad (6)$$

The length h is interpreted as the width of an elastic influence zone around the fracture zone. Ulfkjaer et al. (1995) found that for bending of a beam $h=D/2$ gives a satisfactory correspondence with FEM based calculations, however, a more sophisticated model is suggested later in the present paper.

When $B=0$, the material acts as elastic-plastic and when $B=1$ it becomes perfectly elastic-brittle. The brittleness number includes both the material fracture energy and the structural size, thus, a high number is obtained by either small fracture energy and/or large size.

The situation $B=0$ corresponds to the total elongation and the fracture zone elongation being identical. In the opposite situation $B=1$ the material fracture zone cannot dissipate the elastic energy and the failure is sudden. Note that in case of large values of h the numerical value of B may exceed unity, which is of course meaningless. However, in this case the upper limit $B=1$ is applied.

3 BENDING ANALYSIS

A rectangular cross-section of thickness t and depth D is analysed and the Bernoulli-Navier assumption is applied. The cross-section is subjected to a curvature κ (Fig. 2). Both Chuang & Mai (1989) and Ulfkjaer et al. (1995) have solved the bending problem analytically. The former used the smeared crack band model and the latter the fictitious crack model. Furthermore, Chuang & Mai applied a general power-law softening curve while Ulfkjaer et al. analysed a linear curve. Here we adopt the solution scheme provided by Ulfkjaer et al. (1995) but it is emphasized that both solutions yield basically the same result despite slightly different normalisations.

It is noted that Chuang & Mai (1989) did not recognize any size-effect on the modulus of rupture because they implicitly assumed $h=h_c$ in Equation 5 and thus, the width of the elastic influence zone was treated as a material property.

The modulus of rupture is defined as

$$f_r = \frac{6M_u}{tD^2} \quad (7)$$

where M_u = ultimate bending capacity.

Before the ultimate capacity is reached the cross-section behaves as linear-elastic in accordance with the following non-dimensional equation

$$\begin{aligned} M(\kappa) &= \frac{tD^3}{12} E\kappa \Leftrightarrow \\ m(\theta) &= \frac{6M(\kappa)}{f_t t D^2} = \frac{D\kappa}{2\varepsilon_i} = \theta \end{aligned} \quad (8)$$

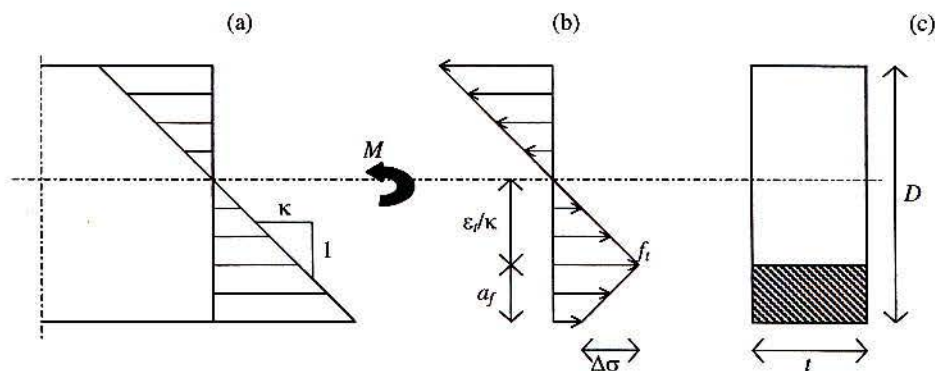


Figure 2. Beam cross-section, (a) strains, (b) stresses and (c) geometry. The hatching symbolises the fictitious crack.

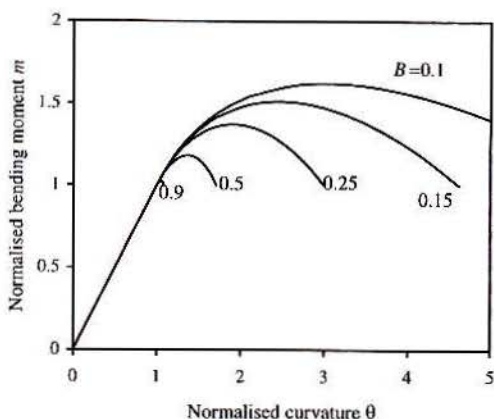


Figure 3. Examples of m - θ curves with various B . The end points of the curves correspond to θ_c .

3.1 Softening of the fracture zone

The softening of the tensile fibre starts when $m(\kappa)=1$ (i.e. when $D\kappa=2\varepsilon_t$ in Equation 8 and a fracture zone of depth a_f starts to grow (Fig. 2). For a given curvature, balancing the compressive and tensile stresses over the cross-section yields the extension of the fracture zone. The following equation is easily obtained

$$D\kappa(1-\alpha_f)^2 - 2\varepsilon_t + \frac{\Delta\sigma}{E}\alpha_f = 0, \quad \alpha_f = \frac{a_f}{D} \quad (9)$$

where E and ε_t are given in Figure 1 and $\Delta\sigma$ represents the drop in tensile stress at the outermost fibre, defined as

$$\Delta\sigma = f_t - \sigma(w) = ED\kappa\alpha_f \frac{B}{1-B} \quad (10)$$

where Equations 4 and 5 are applied. For the crack band model $\Delta\sigma$ reads the same, as a result of the previous definition of B . Inserting Equation 10 in 9 the parabolic equation presented by Ulfkjær et al. (1995) is obtained, which is to be solved for α_f

$$\frac{\alpha_f^2}{1-B} - 2\alpha_f - \left(\frac{1}{\theta} - 1\right) = 0, \quad \theta \geq 1 \quad (11)$$

where the normalised curvature θ from Equation 8 is inserted. Expressions for α_f and the bending moment are taken from Ulfkjær et al.:

$$\alpha_f = 1 - B - \sqrt{(1-B)(1/\theta - B)}$$

$$m(\theta) = \theta \left(\frac{2\alpha_f^3}{1-B} - 6\alpha_f + 4 \right) - 3, \quad \theta \geq 1 \quad (12)$$

See Figure 3 for a few examples of the m - θ curves.

The above expressions are valid as long as the fracture zone has not softened completely, i.e. until $\Delta\sigma$ in Equation 10 reaches f_t , corresponding to

$$\Delta\sigma = f_t \Leftrightarrow \theta_c = \frac{1+\sqrt{B}}{2B} \quad (13)$$

When the curvature exceeds θ_c the "real" crack starts to grow, however this solution is not pursued here, see Chuang & Mai (1989) and Ulfkjær et al. (1995).

The following limit cases are found:

1 For $B \rightarrow 0$ one finds $\alpha_f \rightarrow 1 - \theta^{-1/2}$ and $\theta_c \rightarrow \infty$. The derivative $dm/d\theta \rightarrow \theta^{-3/2}$ of the m - θ curve is always positive.

Thus, the peak of the m - θ curve is calculated as $m(\theta \rightarrow \infty, B=0) = 2(3 - \theta^{-1/2}) - 3 = 3$, being the well known asymptotic elastic-plastic small-size behaviour, see e.g. Olsen (1994).

2 For $B \rightarrow 1$ one obtains $\alpha_f \rightarrow 0$ and at the peak moment it is found numerically that $\alpha_f(1-B) \rightarrow 1/4$. Thus, the peak value of m equals 1 in this case. These asymptotic values for the modulus of rupture are identical to those applied by Planas et al. (1995).

4 MODULUS OF RUPTURE

From the expressions in Equation 12, the bending moment versus curvature is obtained. The peak value of m is by definition equal to the ratio between the modulus of rupture and the tensile strength f_t/f_t . It can be found by differentiation of Equation 12, but no analytical closed form solution has been obtained.

From comparisons with FEM based calculations on beams under three-point bending Ulfkjær et al. (1995) concluded that $h=D/2$ is a plausible value in order to obtain agreement on the complete load-deflection curves and not just on the peak load. Applying this simple model on Equation 6 the brittleness number equals

$$B = \frac{h}{2l_1} = \frac{1}{4} \frac{D}{l_1} \quad (14)$$

In Figure 4 the f_t/f_t values obtained from the peak values of Equation 12 are depicted as a function of D/l_1 defined in Equation 14. Furthermore, the extension of the fracture zone and the normalised stress drop is shown. The fracture zone is seen to approach unity for small-size (plastic) behaviour and zero for large-size behaviour. The stress drop $\Delta\sigma$ is seen to increase continuously from zero to $f_t/2$ within the same range. This is contrary to what Planas et al. (1995) reported, viz. $\Delta\sigma$ increasing with D/l_1 to a maximum of approximately $f_t/3$ at $D/l_1=0.5$ followed by a decreasing $\Delta\sigma$.

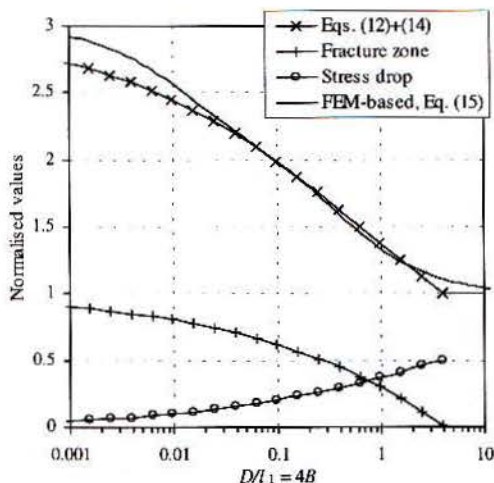


Figure 4. Modulus of rupture, f_r/f_i versus D/l_1 and corresponding α_f/D and $\Delta\sigma/f_i$. Note semi logarithmic scale.

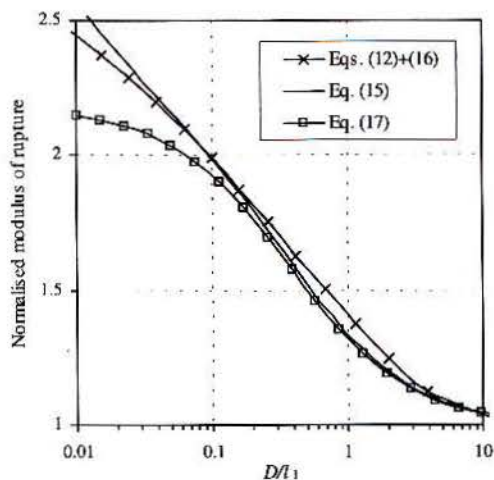


Figure 5. Modulus of rupture, f_r/f_i versus D/l_1 .

Planas et al. (1995) provided a general expression, based on FEM calculations, accommodating both small- and large-size asymptotic behaviour (Fig. 4):

$$\frac{f_r}{f_i} = \beta + \frac{3 - \beta + 99 D/l_1}{(1 + 2.44 D/l_1)(1 + 87 D/l_1)} \quad (15)$$

where β = constant taking into account that not pure bending conditions exist. However, in the present analysis $\beta=1$ is applied. The difference between Equations 15 and 12 in Figure 4 is mainly due to the rather crude assumption in Equation 14 giving an abrupt change in the behaviour of Equation 12 at $D/l_1=4$ ($B=1$) whereas Equation 15 models a smooth asymptotic large-scale behaviour. In order to avoid this abrupt change an exponential relationship between B and D/l_1 is suggested:

$$B = 1 - \exp\left\{-\frac{1}{4} \frac{D}{l_1}\right\} \Leftrightarrow \frac{D}{l_1} = -4 \ln\{1 - B\} \quad (16)$$

where the correct asymptotic behaviour is maintained. The result of combining Equation 16 with Equation 12 is shown in Figure 5.

The $B-D/l_1$ relationship of Equation 16 is depicted in Figure 6. The definition $B=h/(2l_1)$ implies that the slope of the $B-D/l_1$ relationship is proportional to the ratio h/D , i.e. h/D decreases with increasing D .

Planas et al. (1995) also discuss several simplified expressions having various degrees of accuracy. Basically these are of the form originally suggested by Hillerborg and co workers (Fig. 5):

$$\frac{f_r}{f_i} = \beta + \frac{\beta}{0.85 + 2.3 D/l_1} \quad (17)$$

where the constants in the denominator are fitted to FEM results. Generally these simplified models are found plausible for the large-size behaviour and fail to model the small-size asymptotic behaviour. Furthermore, Planas et al. (1995) discuss the approximate expression given by Bazant & Li (1995) together with the Jenq & Shah two-parameter-model and Carpinteri's multifractal law. However, these models are not treated in the present analysis.

5 PRACTICAL APPLICATIONS

In the previous sections l_1 is considered to be a material property, governed by the initial part of the tensile softening curve. The question is now: what is the value of l_1 for practical concrete mixes?

The CEB-FIP Model Code (1991) has recommendations for the tensile properties of concrete. The Model Code recommends a bi-linear $\sigma-w$ curve where the area under the curve depends on the grade of concrete and the aggregate size, see also Bazant & Planas (1998), Section 7.2. Using the initial part of this curve l_1 is obtained as 50-60 % of the Hillerborg characteristic length l_{ch} .

In Figure 6 the range of D/l_1 is depicted for typical beam sizes for two different concretes. If a typical laboratory beam-size of 100-200 mm is considered, it is seen that D/l_1 is above 0.3 corresponding to the interval where the size-effect is most pronounced, cf. Figure 5.

5.1 Code of practice

Knowledge of the size-effect of the modulus of rupture is only included in a few concrete codes of practice for design (Fig. 7). The tensile bending strength of plain concrete is of course not used extensively as the beams normally are reinforced with steel. However, the modulus of rupture is for instance used to define the minimum reinforcement requirement by

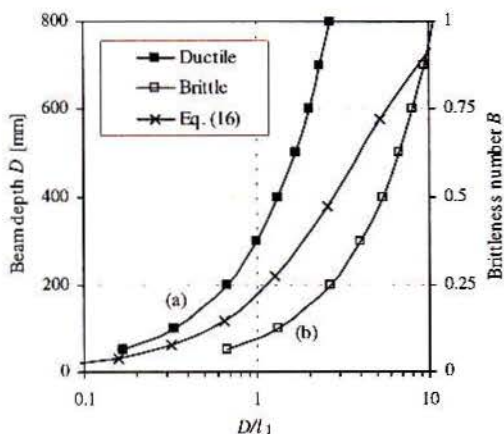


Figure 6. D versus D/l_1 : (a) $l_{cr}=600$ mm and (b) $l_{cr}=150$ mm.

ensuring that the tensile reinforcement is capable of carrying the cracking moment of a beam. The Danish concrete code of practice DS 411 (1999) uses $f_r=2f_t$ to define the minimum reinforcement, which is a rather conservative estimate (Fig. 5). There have been several investigations including the size-effect in the minimum reinforcement requirements for concrete beams. However, this subject is beyond the scope of the present paper, the reader is referred to Bosco et al. (1990) and Bazant & Planas (1998).

In Figure 7 the size-effect expressions adopted by DS 411 (1999) and the CEB Model Code (1991) are depicted along with the analytical solution in the present paper. DS 411 utilizes $D^{-0.25}$ proportionality and the Model Code applies $D^{0.7}$. The latter obviously captures the size-effect better than the former.

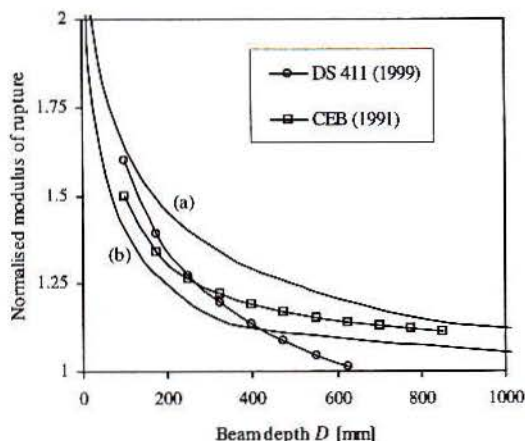


Figure 7. Size-effect comparison between codes of practice and analytical model: (a) $l_1=250$ mm and (b) $l_1=100$ mm.

6 CONCLUSIONS

An analytical bending analysis of rectangular plain concrete beams is presented. It is shown how the fictitious crack model and the crack band model yield identical solutions. The conclusions are:

- 1 Expressions for the bending moment and the depth of the fracture zone are given, based on the Bernoulli-Navier assumption. These expressions depend on a single brittleness number B , including the beam size and the material softening behaviour.
- 2 By choosing a simple dependency between B and the beam depth D , an excellent agreement with FEM-based expressions for the modulus of rupture is obtained. Furthermore, the correct asymptotic behaviour for plastic small-size behaviour and brittle large-size behaviour is obtained.
- 3 The analytical solution includes expressions for the stress distribution and the size of the fracture zone.

REFERENCES

- Alvaredo, A.M. & Torrent, R.J. 1987. The effect of the shape of the strain-softening diagram on the bearing capacity of concrete beams. *Materials and Structures* (RILEM) 20: 448-454.
- Bazant, Z.P. & Oh, B.H. 1983. Crack band theory of concrete. *Materials and Structures* (RILEM) 16(93): 155-177.
- Bazant, Z.P. & Planas, J. 1998. *Fracture and Size Effect in Concrete and other Quasibrittle Materials*. Boca Raton, USA: CRC Press.
- Bazant, Z.P. & Li, Z. 1995. Modulus of rupture: size effect due to fracture initiation in boundary layer. *Journal of Structural Engineering* (ASCE) 121(4): 739-746.
- Bosco, C., Carpinteri, A. & Debernardi, P.G. 1990. Minimum reinforcement in high-strength concrete. *Journal of Structural Engineering* (ASCE) 116(2): 427-437.
- CEB 1991. *CEB-FIP Model Code 1990, Final Draft*. Lausanne, Switzerland: Comite Euro-International du Beton.
- Chuang, T. & Mai, Y.-W. 1989. Flexural behavior of strain-softening solids. *International Journal of Solids and Structures* 25(12): 1427-1443.
- DS 411. 1999. *Code of practice for the structural use of concrete*. (in Danish) Copenhagen, Denmark: Dansk Standard.
- Hillerborg, A., Modeer, M. & Petersson, P.-E. 1976. Analysis of crack formation and crack growth in concrete by means of fracture mechanics and finite elements. *Cement and Concrete Research* 6(6): 773-782.
- Neville, A.M. 1995. *Properties of Concrete*. 4th edition, Harlow, England: Longman Group Ltd.
- Olsen, P.C. 1994. Some comments on the bending strength of concrete beams. *Magazine of Concrete Research*. 46(168): 209-214.
- Planas, J., Guinea, G.V. & Elices, M. 1995. Rupture modulus and fracture properties of concrete. In F.H. Wittmann (ed.), *Fracture Mechanics of Concrete Structures; Proc. FraM-CoS-2: 95-110*. Freiburg, Germany: Aedificatio Publishers.
- Ulfkjaer, J.P., Krenk, S. & Brincker, R. 1995. Analytical model for fictitious crack propagation in concrete beams. *Journal of Engineering Mechanics*. (ASCE) 121(1): 7-15.